Subcellular Imaging of Dynamic Protein Interactions by Bioluminescence Resonance Energy Transfer

Vincent Coulon,*† Martin Audet,‡ Vincent Homburger,* Joël Bockaert,* Laurent Fagni,* Michel Bouvier,‡ and Julie Perroy*

*Institut de Génomique fonctionnelle, CNRS UMR5203, INSERM U661, University of Montpellier, Montpellier, France; †Laboratoire de Dermatologie Moléculaire-EA3754, UFR Médecine Site NORD UPM/IURC, Montpellier, France; and ‡Department of Biochemistry and Groupe de Recherche Universitaire sur le Médicament, Institute of Research in Immunology and Cancer, Université de Montréal, Montréal, QC, Canada

ABSTRACT Despite the fact that numerous studies suggest the existence of receptor multiprotein complexes, visualization and monitoring of the dynamics of such protein assemblies remain a challenge. In this study, we established appropriate conditions to consider spatiotemporally resolved images of such protein assemblies using bioluminescence resonance energy transfer (BRET) in mammalian living cells. Using covalently linked *Renilla* luciferase and yellow fluorescent proteins, we depicted the time course of dynamic changes in the interaction between the V2-vasopressin receptor and β-arrestin induced by a receptor agonist. The protein-protein interactions were resolved at the level of subcellular compartments (nucleus, plasma membrane, or endocytic vesicules) and in real time within tens-of-seconds to tens-of-minutes time frame. These studies provide a proof of principle as well as experimental parameters and controls required for high-resolution dynamic studies using BRET imaging in single cells.

INTRODUCTION

Protein functions rely on their ability to engage in specific protein-protein interactions and to form complexes that are dynamically regulated by stimuli. Several approaches have therefore been developed to study the occurrence and dynamic of protein-protein interactions in living subjects (1). Among them, resonance energy transfer (RET) technologies are becoming increasingly popular. This is in part a result of the development of numerous fluorescent and luminescent organic molecules or proteins amenable to RET and readily usable in biological systems (2). More importantly, fluorescence (FRET) or bioluminescence resonance energy transfer (BRET) allows us to study real-time interactions among proteins expressed in their correct location, in living systems (3–5). FRET and BRET are proximity-based assays that rely on the nonradiative transfer of energy between donor and acceptor molecules according to the Förster mechanism. The efficacy of the energy transfer depends primarily on *1*), the overlap between the emission and excitation spectra of the donor and acceptor molecules, respectively, and *2*), the close proximity and orientation of the donor and acceptor entities (6,7). It varies inversely with the sixth power of the distance and cannot occur for distances exceeding 100 Å for most RET partners currently used. This absolute distance dependence between donor and acceptor makes it possible to monitor protein-protein interactions by attaching RET-compatible donor and acceptor molecules to the proteins studied. In FRET, donor and acceptor are both fluorescent molecules, and thus initiation of the energy transfer requires the excitation of the donor fluorophore by an external light. For BRET, the energy donor is a bioluminescent molecule that emits energy on addition of an organic substrate. One significant advantage of BRET over FRET resides precisely in the fact that no external light excitation is required to initiate BRET. Consequently, BRET circumvents cell autofluorescence, direct excitation of the acceptor fluorophore by external excitation light, or donor fluorophore photobleaching. This results in a higher signal/background ratio and facilitates analysis of the signals generated, making BRET a technology of choice for measurements using microplate readers (8).

Despite the excellent signal/background ratio provided by BRET, the low level of light emission intrinsic to the bioluminescent luciferase reaction and the lack of sensitivity of the cameras classically used for microscopy studies have hampered the use of BRET for the localization of protein complexes at the subcellular level (9). Until recently, FRET was the only RET approach that allowed dynamic study of the subcellular distribution of protein complexes. Unfortunately, the limitations of FRET also apply to microscopy studies. In particular, the acceptor fluorophore is directly excited, and there is bleed-through of the donor fluorescence into the acceptor detection channel, making it difficult to quantify the FRET efficiency precisely, especially when the local stoichiometry of the donor and acceptor are not known and their relative contributions to background signals are difficult to assess (10–12). In addition, the use of an external light source may complicate certain types of experiments as a result of phototoxicity or the undesirable activation of photosensitive biological processes (13). Because use of BRET instead of FRET circumvents many of these difficulties, the

Submitted July 12, 2007, and accepted for publication September 24, 2007.

Address reprint requests to Julie Perroy, IGF, 141 rue de la Cardonille, 34094 Montpellier Cedex 05, France. Tel.: 33-467142960; Fax: 33-467542432; E-mail: julie.perroy@igf.cnrs.fr.

Editor: Petra Schwille.

© 2008 by the Biophysical Society

0006-3495/08/02/1001/09 $2.00

doi: 10.1529/biophysj.107.117275

development of BRET-based microscopy offers complementary approaches that increase our ability to study the spatiotemporal dynamics of protein interactions in living cells. Today, the enhanced sensitivity of microscopy, electron-multiplying cooled charge-coupled device (EMCCD) cameras, and improved bioluminescence probes facilitate luminescence imaging at the single-cell level (14). Because it does not require illumination, bioluminescence imaging circumvents phototoxicity and thereby improves imaging in living subjects (15). Thanks to these recent advances in physics, BRET experiments were recently performed at the cellular level in plant seedlings. In these experiments, the weak light derived from bioluminescence did not photobleach the sample or cause autofluorescence, a particularly acute issue in plant cells because of the presence of chlorophyll (16). Finally, using an improved BRET strategy, De et al. imaged protein interactions in a single line cell and cells located deep within small living subjects (17). This work went further in the development of BRET imaging by establishing the appropriate experimental conditions to visualize and quantify dynamics of protein-protein interactions at the subcellular level in single mammalian cells.

MATERIAL AND METHODS

Plasmids

The pDsRed-N1 plasmid was obtained from Clontech (Mountain View, CA). We used the plasmid ph*R*luc from BioSignal Packard (Meriden, CT) to construct the plasmids coding for the different fusions. The fusion plasmids ph*R*luc-EYFP and ph*R*luc-EGFP$_2$ were generated as previously described (18). In these constructs, the *Renilla* luciferase (*R*luc) is fused to the fluorescent protein variant with a 26-amino-acid linker (GDLASSREFSRV-CRISGARSVLKLGA). The ph*R*luc-EYFP-NLS plasmid was obtained by introducing a sequence coding for a Nuclear Localization Signal PKKKRKV (19) within ph*R*luc-EYFP between the ApaI and BamHI restriction sites, in frame with the C-terminus coding sequence of *R*luc-EYFP. The construction of pcDNA3.1-*R*luc-β-arr2 and pRK5-V2RYFP was previously described (20). The R393E and R395E mutations were inserted using PCR site-directed mutagenesis to obtain the *R*luc-β-arr2(R393E, R395E) construct.

HEK293 cell culture and transfection

HEK293 cell culture and transfection were previously described (21). For experiments using the fusion constructs, distinct pools of cells were transfected with ph*R*luc-EYFP alone or with ph*R*luc-EGFP$_2$ and pDsRed-N1 (transfection reporter). Twenty-four hours after transfection, the two populations of transfected cells were pooled and cultured for an additional 24 h in glass-bottom culture dishes (P35GC-0-14-C, MatTek, Ashland, MA).

BRET measurements in cell population using a spectrophotometric plate reader

Cell population BRET measurements were previously described (20).

BRET imaging

BRET imaging studies were performed using a dedicated Axiovert 200M inverted fluorescence microscope (Zeiss, Jena, Germany) in which all luminescent diodes were taken off and the light source was deviated with an optical fiber 1.5 m long to limit light interference. The microscope was installed in a black box, impermeable to environmental light pollution. All images were obtained with a Plan-Apochromat 63×/1.40 Oil M27 objective at room temperature. First, transfected cells were identified using a monochromatic light and appropriated filters to excite or GFP (exciter HQ480/40 No. 44001, emitter HQ525/50 No. 42017, Chroma, Rockingam, VT) and DsRed (exciter HQ540/40 No. 59313, emitter HQ600/50 No. 65886, Chroma). The light source was then switched off until the end of the experiment. Coelenterazine H (CoelH, 20 μM) was applied 10 min before acquisition except when indicated otherwise. Images were collected using a cascade 512B camera (equipped with an EMCCD detector, back-illuminated, On-chip Multiplication Gain) from Photometrics (Tucson, AZ), mounted on the base port of the microscope. Sequential acquisitions of 30 s (except when specified otherwise in the text) were performed at 5 MHz, gain 3950, binning 1, with emission filters D480/60 nm (No. 61274, Chroma) and HQ535/50 nm (No. 63944, Chroma) to select em480 and em535 wavelengths, respectively. The acquisition software was Metamorph (Molecular Devices, Sunnyvale, CA). To determine the average intensity of em480 and em535 (or later 535 nm/480 nm ratio), we calculated the mean intensity for each image of pixels within a square region drawn on the cell of interest using Image J software (NIH). The signal/background ratio corresponds to the previous average intensity signal over the mean background signal recorded in an adjacent equal surface without cells. The background value (from a cell-free region) was subtracted from the em480 and em535 raw images. A subsequent median filter was applied to obtain the em480 and em535 illustration images of the figures. It is important to note that this treatment reduced the noise in the active image by replacing each pixel with the median of the neighboring pixel values. Therefore, the median filter masked isolated pixels with ratio values in areas with near-background luminescence, which tend to be highly variable or even undefined (division by zero). The pixel-by-pixel 535 nm/480 nm ratios were calculated by dividing the absolute blue or yellow intensities per pixel of images obtained at 535 nm over 480 nm. These numerical ratios (between 0 and 1.5) were translated and visualized with a continuous 256-pseudocolor look-up table as displayed in the figures. Table 1 defines all the variables used to perform BRET imaging. To follow *R*luc-β-arr recruitment to the stimulated V2R-YFP receptor (see Fig. 5, *m* and *n*), CoelH 20 μM was applied 10 min before the first image acquisition, whereas AVP 1 μM was added immediately after the first acquisition. We performed 10 sequential acquisitions of 30 s in each channel every 2 min for 20 min of agonist stimulation.

TABLE 1 Definition of the variables used to perform BRET imaging

Terminology	Definition
em480	Light emission at 450–510 nm, corresponding to *R*luc emission peak at 480 nm.
em535	Light emission at 510–560 nm, corresponding to the YFP emission peak at 535 nm
535 nm /480 nm ratio	Pixel-by-pixel ratio calculated by dividing the absolute intensities per pixel of images obtained at 535 nm over 480 nm
Average intensity	Mean intensity of pixels within a square region drawn on the cell of interest before image analysis
Background	Mean intensity of pixels within a square region drawn in a surface without cells before image analysis
Signal/background	Ratio corresponding to the previous average intensity signal over the background signal recorded in two adjacent equal surfaces
Basal 535 nm/480 nm ratio	535 nm/480 nm ratio obtained in the presence of *R*luc and absence of acceptor entity. Corresponds to the overflow of the *R*luc output into the YFP acceptor detection channel

Statistical analysis

The distribution of median 535 nm/480 nm ratios for each cell was analyzed using Kaleidagraph software. Statistical analyses on 535 nm/480 nm ratios distribution (medians and quartiles) were performed with the nonparametric Kruskal-Wallis test for more than two independent samples with a risk threshold of 5%.

RESULTS

Validation of the BRET technology to image protein-protein interactions

In BRET, the catalytic oxidation of Coelenterazine H (CoelH) by the bioluminescent enzyme *R*luc results in the emission of light with a peak at 480 nm. When an appropriate energy acceptor such as the yellow fluorescent protein (YFP) is present within RET-permissive distances of *R*luc, part of the energy can be transferred nonradiatively, leading to the excitation of the YFP and emission of light at its characteristic wavelength with a peak at 530 nm (22). In a first attempt to detect BRET signals by microscopy, we took advantage of an artificial protein directly linking *R*luc to YFP through an amino acid linker of 26 amino acids. This chimeric protein generates large BRET signals that were detected using spectrometric plate readers (Fig. 1) and was thus used as a positive model.

One of the major difficulties in establishing RET imaging is to distinguish the signal originating from the transfer of energy from that resulting from an overflow of the energy donor output into the energy acceptor detection channel. To control for this basal signal, we used another chimeric protein linking *R*luc to a distinct green fluorescent protein (GFP) variant, GFP_2, which displays a maximum excitation peak at 400 nm (23) but cannot be efficiently excited at 480 nm (wavelength corresponding to *R*luc peak emission). As shown in Fig. 1, the signal detected in cells expressing *R*luc-GFP_2 on addition of CoelH was not different from that observed in cells expressing *R*luc alone, indicating that it corresponded to the overflow donor emission: basal 535 nm/480 nm ratio. Thus, this *R*luc-GFP_2 fusion, almost identical to *R*luc-YFP, but incapable of any energy transfer in the presence of CoelH, was a stringent negative BRET control in the following BRET imaging experiments. *R*luc-GFP_2 was cotransfected with the DsRed used as a transfection reporter to identify cells that do not display BRET. Another pool of cells was transfected in parallel with *R*luc-YFP to obtain the positive BRET cells. Those two populations of transfected cells were subsequently mixed (24 h after transfection). Because of the DsRed, cells expressing *R*luc-YFP or *R*luc-GFP_2 + DsRed could therefore be identified when studied in the same microscopic field (Fig. 2, *a* and *b*), allowing a direct comparison of cells that do or do not display BRET. The emission of light at 450–510 nm (corresponding to the *R*luc emission peak at 480 nm, em480) and 510–560 nm (corresponding to the YFP emission peak at 535 nm, em535) were acquired sequentially every 30 s, 10 min after the addition of CoelH (Fig. 2, *c* and *d*). The ratio of images obtained at 535 nm to those obtained at 480 nm (535 nm/480 nm, see Methods) revealed strong signals in cells expressing *R*luc-YFP, whereas only marginal signals were observed in cells expressing the BRET-negative control *R*luc-GFP_2 (Fig. 2 *e*), indicating that BRET originating from *R*luc-YFP was detected at the single-cell level.

Kinetics of the BRET signal

To determine the optimal acquisition time after addition of CoelH, we recorded the em480 and em535 every minute for 1 h with repeated sequential acquisitions of 30 s at each wavelength. The em480 signal could be detected as early as 5 min after the addition of CoelH, reached its maximum between 15 and 20 min after the addition of the *R*luc substrate, and gradually declined afterward (Fig. 2, *f* and *g*). Because the intensity of the em480 depends on the expression level of the *R*luc protein, cells displayed various intensities of em480 (Fig. 2 *g*). The em535 displayed similar kinetics and was also dependent on the expression level of the fusion proteins. As expected, however, similar levels of em480 (compare cells 3 and 4) yielded much higher em535

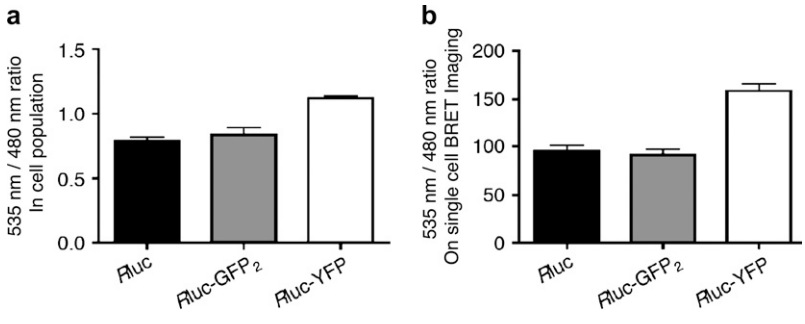

FIGURE 1 *R*Luc-GFP_2 fusion as a stringent negative control to determine the 535 nm/480 nm signal originating from the overflow of the energy donor output into the energy acceptor detection channel. Cells transfected with the soluble *R*luc or *R*luc-YFP fusion or *R*luc-GFP_2 construct were incubated in the presence of CoelH 10 min before measurement of em480 and em535 in (*a*) a spectrophotometric plate reader or (*b*) under microscope. Data are means ± SE of three independent experiments (plate reader) or means ± SE of 10 or 15 cells for each transfection condition (BRET imaging). Note that in both experiments the 535 nm/480 nm signal obtained in cells transfected with the *R*luc-GFP_2 construct is not significantly different from the one obtained in cells expressing the soluble *R*luc, thus validating the use of the *R*luc-GFP_2 construct as a stringent negative control to measure the basal 535 nm/480 nm ratio (i.e., 535 nm/480 nm ratio obtained in absence of BRET acceptor). In *b*, the original numerical 535 nm/480 nm ratios (between 0 and 1.5) were converted to a scale ranging from 1 to 256. This translation allows us to visualize the 535 nm/480 nm ratios with a continuous 256 pseudocolor look-up table, as displayed in subsequent figures.

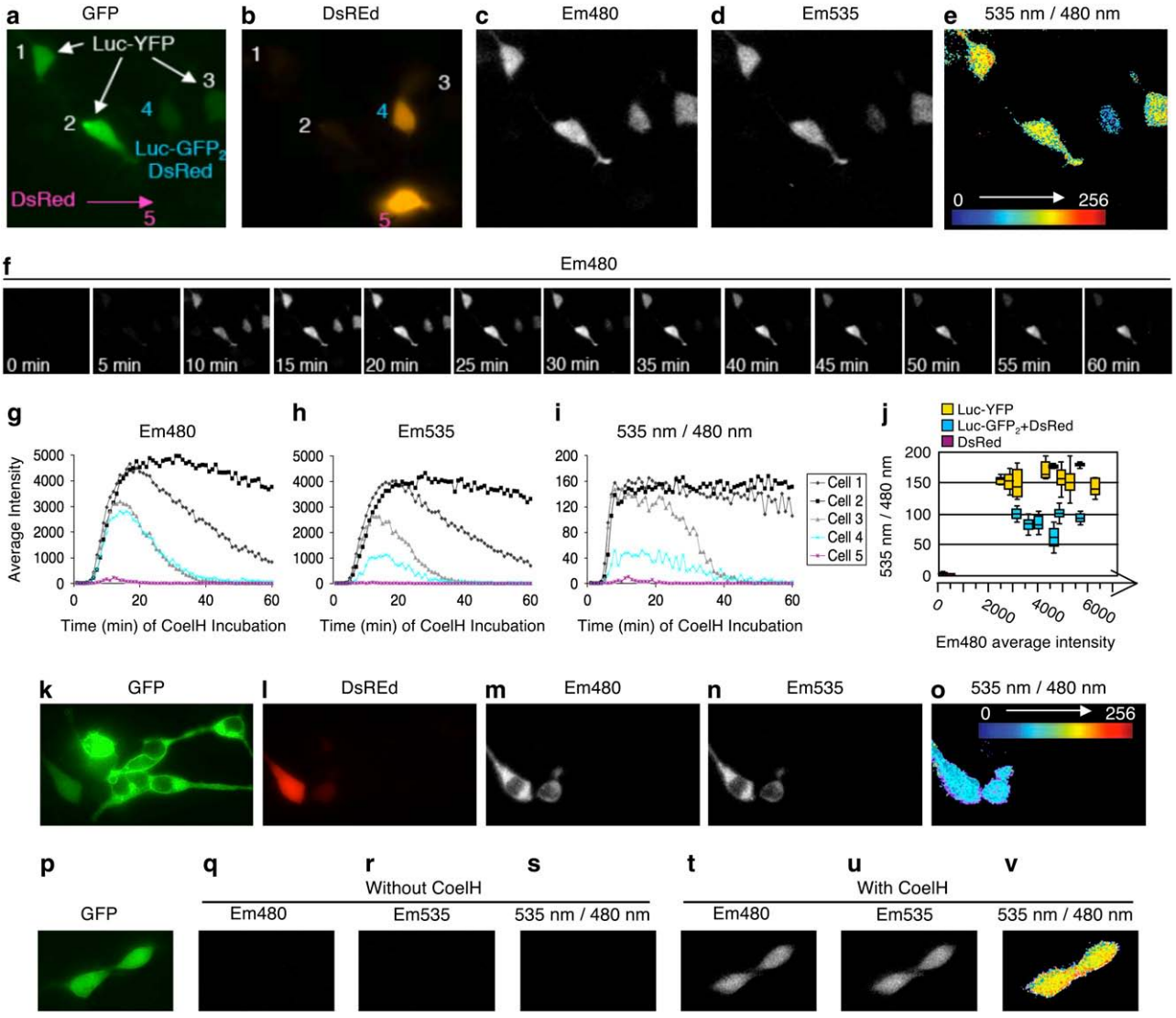

FIGURE 2 The em480, em535, and 535 nm/480 nm images. (*a*) YFP fluorescence comparison with (*b*) DsRed fluorescence was used to discriminate among cells expressing *R*Luc-YFP (*cells 1, 2*, and *3*), *R*LucGFP$_2$/DsRed (*cell 4*), or DsRed alone (*cell 5*). Sequential acquisition (30 s each) of (*c*) em480 and (*d*) em535 recorded 10 min after the addition of 20 μM CoelH. (*e*) 535 nm/480 nm ratio images (derived from *d*/*c*) presented in pseudocolors. (*f*) Images of em480 acquired every 5 min from 0 to 60 min after CoelH application. Intensities of (*g*) em480, (*h*) em535, and (*i*) 535 nm/480 nm signals over 1 h after CoelH application. (*j*) Boxes illustrating the median and dispersion of the maximal 535 nm/480 nm ratio intensities (10 min after addition of CoelH) for independent cells expressing Luc-YFP (nine cells) or Luc-GFP$_2$ + DsRed (six cells) or DsRed (two cells). Each value was obtained by determining the 535 nm/480 nm ratio for each pixel within a square of 21 $\times$ 21 pixels in the middle of the cell. The axes indicate the em480 level (indicative of the fusion protein amount) of each independent cell analyzed. (*k*) YFP fluorescence comparison with (*l*) DsRed fluorescence was used to discriminate between *R*Luc-negative cells expressing GFP alone and *R*LucGFP$_2$/DsRed. Sequential acquisition (30 s each) of (*m*) em480 and (*n*) em535 recorded 10 min after the addition of 20 μM CoelH. (*o*) 535 nm/480 nm ratio images (derived from *n*/*m*) presented in pseudocolors. (*p*) YFP fluorescence to identify cells expressing *R*Luc-YFP. Sequential acquisition (30 s each) of (*q* and *t*) em480 and (*r* and *u*) em535 recorded in absence of (*q* and *r*) CoelH or 10 min after the addition of (*t* and *u*) 20 μM CoelH. (*s–v*) 535 nm/480 nm ratio images (derived from *r*/*q* and *u*/*t*, respectively) presented in pseudocolors.

in cells expressing *R*luc-YFP than *R*luc-GFP$_2$ at all times examined (Fig. 2 *h*). Accordingly, the 535 nm/480 nm ratios were greater in cells expressing the positive BRET constructs, reaching their maximum 5 min after addition of CoelH and remaining constant for at least 25 min thereafter (Fig. 2 *i*). Most importantly, the maximal 535 nm/480 nm ratios did not depend on the protein expression level and were identical independently of the em480 intensity detected (compare cells 1, 2, and 3). The 535 nm/480 nm ratios started to decline for acquisition obtained more than 30 min after CoelH addition. The decrease was more pronounced in cells expressing lower protein levels (for exemple, cell 3), most likely reflecting linear detection limits of the em535 that was reached with these low levels of em480 emission. Statistical analyses confirmed significantly higher 535 nm/480 nm ratios in cells expressing *R*luc-YFP (Fig. 2 *j*), allowing a

clear distinction from the population of cells expressing *R*luc-GFP_2. Interestingly the 535 nm/480 nm ratios obtained in cells transfected with the negative BRET control, *R*luc-GFP_2, were also independent of the expression level of the fusion (Fig. 2 *j*).

Because of the high fluorescence quantum efficiencies of YFP, possible traces of light in the black box could lead to image the YFP or CoelH fluorescence rather than BRET. We therefore verified that *1*) *R*luc-negative cells expressing only GFP did not display em480 or em535 signals (Fig. 2, *k–o*), and *2*) *R*luc-positive cells did not emit light at 480 nm and 535 nm before CoelH application (Fig. 2, *p–v*). These are stringent controls that we systematically performed with our single photon detection camera.

Temporal resolution of BRET imaging

We next assessed the minimal acquisition time necessary to detect reliable BRET signals. Cells expressing *R*luc-YFP or *R*luc-GFP_2 (Fig. 3, *a* and *b*) were therefore incubated with CoelH for 10 min before sequential acquisition of em480 and em535 for intervals of 1 to 120 s (Fig. 3, *d* and *e*). As expected, the em480 and em535 signals increased linearly with the acquisition time (Fig. 3, *f* and *g*). However, for very short acquisition times (<10 s), the 535 nm/480 nm ratios were out of the linear range, probably because of the camera detection limit. Signal/background ratios were then obtained for em480, em535, and 535 nm/480 nm ratios (see Methods). As shown in Fig. 3 *h*, the signal/background ratio (measured before any treatment of the images), which reflects the image contrast, varied as a hyperbolic function of the acquisition time. For the 535 nm/480 nm ratios, the values reached the asymptote for acquisition time above 20 s, indicating that longer acquisition times are not necessary and would not provide clearer images.

Spatial resolution of BRET imaging

To determine whether BRET imaging could offer the necessary resolution to distinguish among subcellular compartments, a nucleus localization signal (NLS) was attached to *R*luc-YFP (*R*luc-YFP-NLS). Cells transfected with *R*luc-YFP-NLS displayed a BRET signal strictly restricted to the nucleus (Fig. 4, *a–f*), indicating that BRET can readily be imaged in a cellular organelle. Analysis of the median and intensity distribution of 535 nm/480 nm ratios detected in individual cells revealed equivalent 535 nm/480 nm ratios for this nuclear construct (Fig. 4 *g*) as those observed for *R*luc-YFP without NLS (Fig. 2 *j*). This indicated that the nuclear localization did not influence the 535 nm/480 nm ratio, which remained independent of the expression level. Interestingly, on cotransfection of *R*luc-YFP-NLS with *R*luc-GFP_2, the specific nuclear BRET signal could readily be distinguished from the basal 535 nm/480 nm ratio originating from *R*luc-GFP_2 uniformly distributed in the cytoplasm and the nucleus (Fig. 4, *h–l*). A BRET signal originating from a specific subcellular location can thus easily be distinguished from the basal 535 nm/480 nm ratio, even if a protein attached to *R*luc is distributed throughout the cell. This obviously opens the possibility of studying the subcellular localization of specific interactions.

Proof of principle: dynamic recruitment of β-arrestin to the activated vasopressin receptor quantified in space and time by BRET imaging

In an effort to establish whether BRET imaging could be used to monitor dynamic interactions between cellular proteins, we monitored the interaction between V2R and β-arrestin2 (β-arr), a versatile regulatory protein that is actively recruited to many G-protein-coupled receptors only as a result of receptor activation (24). We transfected cells with V2R-YFP and *R*luc-β-arr fusion proteins to image V2R-β-arr interactions by BRET. As expected, in the absence of receptor activation, *R*luc-β-arr was homogeneously distributed throughout the cells, as illustrated by the dispersed em480 signal observed after CoelH addition. Given the lack of basal interaction between V2R-YFP and *R*luc-β-arr, the weak 535 nm/480 nm ratios observed under this control condition most likely reflect the overflow of the *R*luc output into the YFP acceptor detection channel (Fig. 5, *a–c*). Consistent with this deduction, analysis of the mean 535 nm/480 nm ratios intensities in more than 10 individual cells yielded values identical (mean 535 nm/480 nm of 92 ± 8) to the basal 535 nm/480 nm ratios obtained for *R*luc-GFP_2 (mean 535 nm/480 nm of 91 ± 5). In contrast, agonist stimulation of the receptor promoted strong clustering of both em480 and em535, resulting in significant 535 nm/480 nm ratios images that reflect β-arr recruitment to the receptor (Fig. 5, *d–f*). The punctate BRET pattern observed most likely resulted from the trafficking of the V2R/β-arr complex to clathrin-coated pits and endocytic vesicles that can be observed throughout the cells (24). To further test the spatial resolution of BRET imaging, we took advantage of a *R*luc-β-arr mutant in which the C-terminal residues R393 and R395, involved in *R*luc-β-arr's interaction with the endocytic adaptor protein 2 (AP2) are mutated to glutamic acids. The resulting β-arr(R393E,R395E) can still be recruited to the receptor but remains in a more diffuse pattern at the plasma membrane and is found only rarely in clathrin-coated pits (25,26). As shown in Fig. 5, *j–l*, the 535 nm/480 nm ratio images obtained after agonist-promoted recruitment of *R*luc-β-arr(R393E,R395E) could be readily distinguished from those obtained with *R*luc-β-arr (Fig. 5, *d–f*) in that the signal was largely restricted to the plasma membrane in agreement with the subcellular-distribution properties of this mutant form of β-arr.

BRET imaging was then used to monitor the kinetics of *R*luc-β-arr recruitment to the activated V2R-YFP. The em480 and em535 were measured in the same cells before and at intervals of 2 min after the addition of the V2R agonist AVP. As shown in Fig. 5 *m*, the agonist promoted a time-dependent

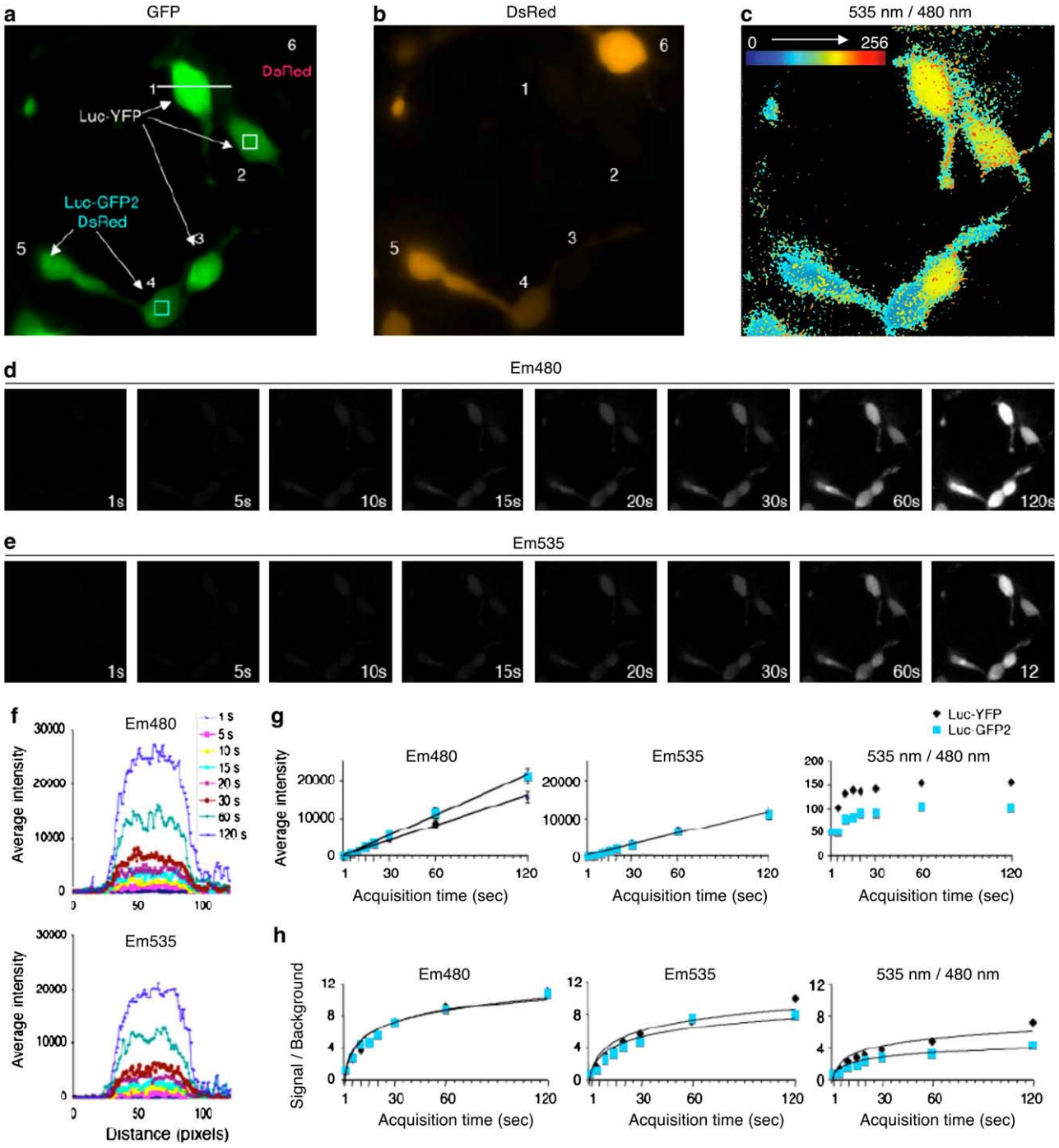

FIGURE 3 Influence of acquisition time for BRET imaging. (*a*) YFP fluorescence comparison with (*b*) DsRed fluorescence was used to discriminate between cells expressing *R*Luc-YFP (*cells 1, 2*, and *3*), *R*LucGFP$_2$/DsRed (*cells 4* and *5*), or DsRed alone (*cell 6*). (*c*) 535 nm/480 nm ratio images derived from 10-s sequential acquisition of em480 and em535 10 min after the addition of CoelH. (*d*) em480 and (*e*) em535 images obtained for acquisition time varying from 1 to 120 s recorded 10 min after the addition of CoelH . (*f*) em480 (*upper panel*) or em535 (*lower panel*) intensities recorded for the indicated acquisition times along a cross-section of cell 1 (*white bar;* 1 pixel = 250 nm). (*g*) Average of em480, em535, and 535 nm/480 nm signal intensities and (*h*) signal/background ratios measured for each pixel in the white and blue squares of 21 × 21 pixels of cells 2 and 4, respectively (drawn in *a*) as a function of acquisition time.

increase in the 535 nm/480 nm ratios that gradually converged into punctuate structures. The stacked histogram representation of the 535 nm/480 nm ratio intensities detected throughout the plane of the cell clearly indicate that the BRET signal reached its maximum after 8 min of stimulation and remained relatively constant at least up to 16 min after AVP addition (Fig. 5 *n*), consistent with the known kinetics of β-arr recruitment to V2R (27). This kinetics of *R*luc-β-arr

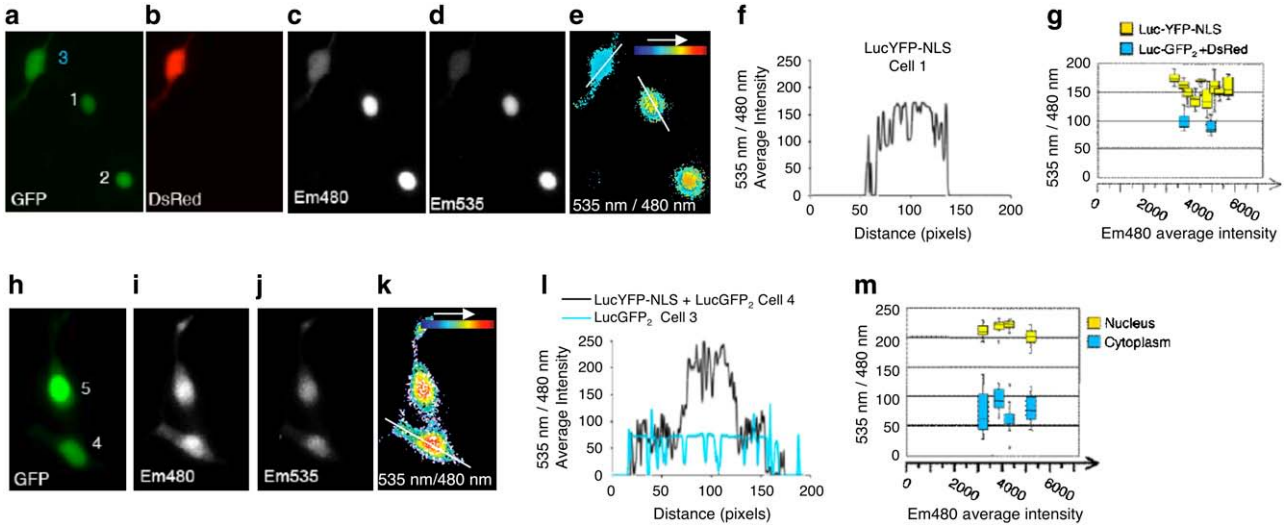

FIGURE 4 Nuclear BRET imaging. (*a*) YFP fluorescence versus (*b*) DsRed fluorescence in cells expressing *R*Luc-YFP-NLS (cells 1 and 2; note the nuclear labeling), *R*LucGFP$_2$/DsRed (cell 3; note the labeling throughout the cell). Sequential acquisition (30 s each) of (*c*) em480 and (*d*) em535 10 min after the addition of CoelH. (*e*) 535 nm/480 nm ratio images (derived from *d*/*c*) presented as pseudocolors. (*f*) 535 nm/480 nm average intensities for a cross-section of cell 1 expressing *R*Luc-YFP-NLS (see *white bar* in *image e*; 1 pixel = 250 nm). (*g*) Boxes illustrating the median and the distribution of the 535 nm/480 nm ratio intensities for independent cells expressing Luc-YFP-NLS (nine cells) or Luc-GFP$_2$ + DsRed (two cells). Each value was obtained from a square of 14 × 14 pixels in the nucleus region of the cell. The axes indicate the em480 level (indicative of the fusion protein amount) of each independent cell analyzed. (*h–k*) Cells were cotransfected with *R*Luc-YFP-NLS and *R*LucGFP$_2$, and fluorescence was measured to identify the expressing cells (*h*). (*i*) Em480, (*j*) em535, and (*k*) 535 nm/480 nm images obtained as above. (*l*) 535 nm/480 nm ratio average intensities for a cross-section of cells 3 and 4 (see *white bar* in *image k* and *blue bar* in *image e*; 1 pixel = 250 nm). (*m*) Illustration of the median and distribution of 535 nm/480 nm ratio intensities measured from squares of 14 × 14 pixels in the nucleus (*yellow squares*) or cytoplasm (*blue squares*) of four independent cells cotransfected with *R*Luc-YFP-NLS and *R*Luc-GFP$_2$.

recruitment to the V2R-YFP measured in a single cell was very similar to that determined by measuring the 535 nm/480 nm ratio in a cell population using a luminofluorometer plate reader (Mithras, Bad Wildbad, Germany) (Fig. 5 *o*). As shown in Fig. 5 *p*, single-cell microscopic BRET imaging also made it possible to generate dose-response curves of the agonist-promoted *R*luc-β-arr recruitment to V2R-YFP, yielding an EC50 for AVP identical to that obtained in cell populations by use of a plate reader.

DISCUSSION

This study provides a proof of principle that BRET can be used to image subcellular protein-protein interaction dynamics in single living cells. We first established the experimental conditions to obtain meaningful BRET images and subsequently depicted the spatiotemporal interaction between the V2R and β-arr in mammalian cells. Coupling a sensitive EMCCD camera to a fluorescence microscope isolated from ambient light pollution is sufficient to detect em480 and em535 signals to obtain 535 nm/480 nm ratio images. The time windows allowing constant BRET values were sufficient to quantitatively monitor biological events in real time within the tens-of-seconds to tens-of-minutes time frame. Acquisition time between 10 and 120 s and images obtained 5 to 30 min after CoelH addition yielded quantitatively accurate values. Obviously, these parameters will need to be established carefully for each detection system used to perform BRET imaging. In that respect, it should be noted that the system used here relied on the sequential acquisition of the em480 and em535 signal images.

An important aspect of the BRET imaging method described herein is the ability to easily distinguish the true energy transfer signal from the basal 535 nm/480 nm ratio, bringing to light the BRET signal originating exclusively from the energy transfer. We also found that for a given donor/acceptor ratio, the BRET values derived from the images are independent of the energy donor expression levels (see Figs. 2 *j* and 4, *g* and *m*), confirming that, as is the case for FRET, BRET imaging offers the quantitative advantage of a ratiometric measurement that is independent of the absolute intensity of the energy donor. Because it is easier to determine the background from BRET than FRET, and, in contrast to FRET, there is no artifactual direct excitation of the energy acceptor, it is easier to take advantage of the independence of RET from the expression level of the energy donor to perform quantitative BRET image analysis.

BRET imaging offers sufficient resolution to detect signals that originate selectively from subcellular compartments (nucleus, plasma membrane, or endocytic vesicles). Indeed, the 535 nm/480 nm signal from the nucleus-targeted *R*luc-YFP-NLS fusion could easily be distinguished from the *R*luc-GFP$_2$ weak signal dispersed throughout the cell. BRET imaging thus allows us to detect interactions between and among proteins exclusively in the compartment where they occur even if the protein attached to the energy donor is

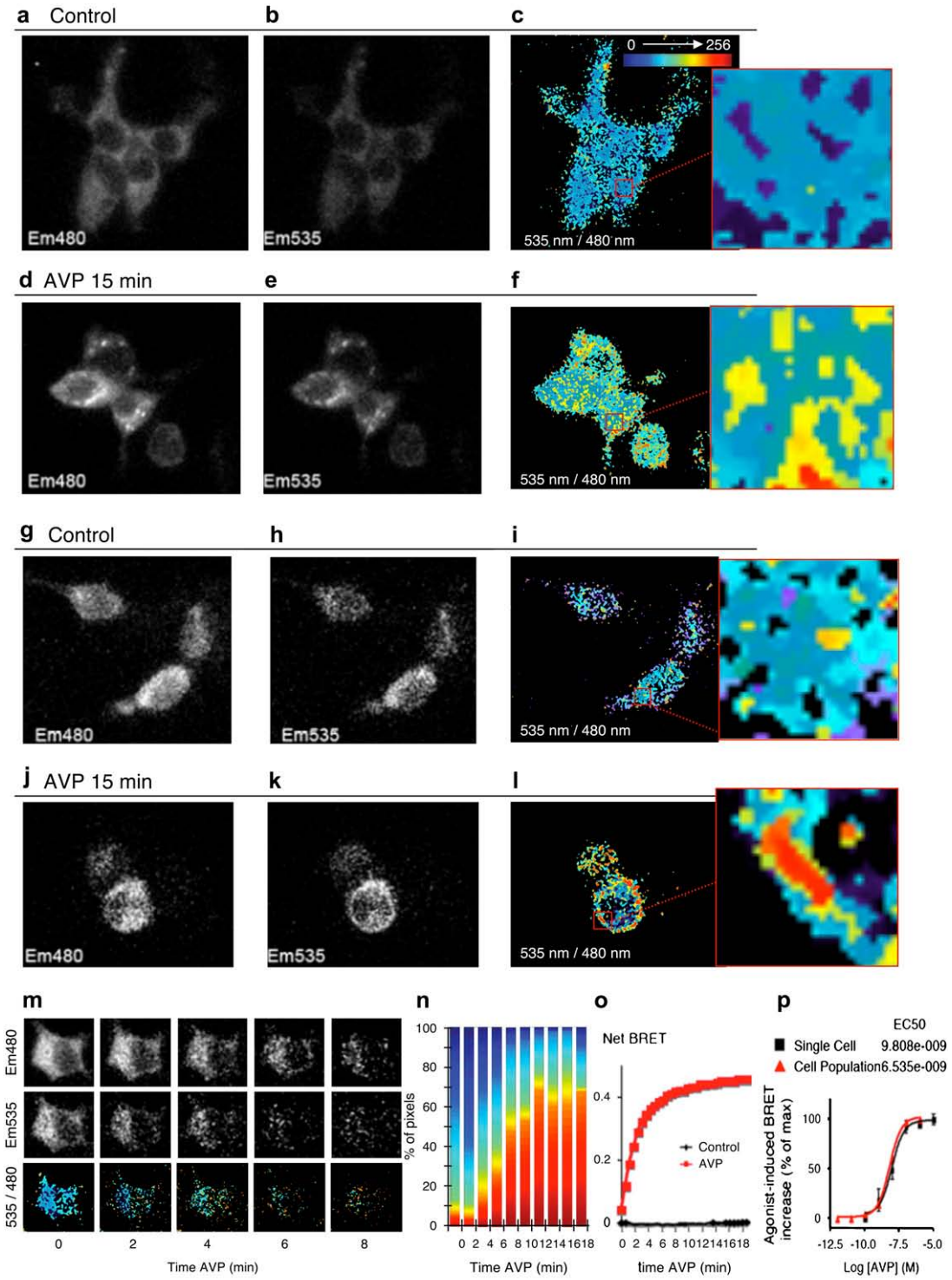

FIGURE 5 BRET imaging of β-arr recruitment to activated V2R. Cells were cotransfected with V2R-YFP and *R*luc-β-arr (*a–f* and *m–p*) or with V2R-YFP and *R*luc-β-arr(R393E,R395E) (*g–l*). (*a–l*) em480, em535, and 535 nm/480 nm images obtained under basal conditions (*a–c* and *g–i*) or after stimulation with 1 μM AVP for 15 min (*d–f* and *j–l*). Right panels of *c*, *f*, *i*, and *l* represent a zoom of the indicated square regions. (*m*) em480, em535, and 535 nm/480 nm images measured in the same cell as a function of time after addition of AVP. Cells illustrating panels *a* to *m* are representative of 5 to 10 similar experiments. (*n*) Normalized stacked histogram of the pseudocolor 535 nm/480 nm values determined in a plane of 21 $\times$ 21 pixels for each time of AVP stimulation in a single cell. (*o*) Kinetics of *R*luc-β-arr recruitment to the stimulated V2R-YFP measured by BRET on a population of cells using a fluoroluminometer plate reader. (*p*) Dose-response curves of AVP-stimulated *R*luc-β-arr recruitment to V2R-YFP determined on a single cell (BRET imaging) or on a cell population (plate reader). Agonist effects were measured 15 min after AVP stimulation. Data represent means $\pm$ SE of three independent experiments (plate reader) or means $\pm$ SE of five to six cells for each AVP concentration (BRET imaging).

widely distributed throughout the cell. This was confirmed in that the BRET signal, originating from the interaction between *R*luc-β-arr and V2R-YFP at the plasma membrane and endocytic vesicles, was distinguished from the overflow signal of the *R*luc-β-arr dispersed in the cytoplasm. Finally, BRET clearly images the dynamic recruitment of β-arr to the V2R on agonist stimulation of the receptor. Highly sensitive, the assay made it possible to quantitatively monitor the kinetic and dose dependence of the recruitment at the single-cell level, yielding half-times and EC50 similar to those obtained from the analysis in cell population (plate readers).

The possibility of imaging BRET signals will undoubtedly increase the breadth of potential applications of the technique. Indeed, identifying the subcellular location of the interaction monitored and quantitatively assessing changes that occur only in specific compartments provide a clear advantage over the classical spectrophotometric BRET analysis obtained from plate readers. Given the limitations of FRET imaging linked to higher and more difficult-to-control backgrounds, possible phototoxic effects of prolonged light illumination, or undesirable activation of photosensitive biological processes, we foresee that BRET imaging will offer an advantageous method that will nicely complement the toolset currently available to study protein-protein interactions in living cells.

We thank A. Carette, M. Vasseur, M. Hogue, and C. Grolleau for technical help, F. Raynaud for critical analyses of the images, and D. Rochdi and D. Michaud for providing *R*luc-β-arr2(R393E, R395E).

This work was supported by the European Community (LSHM-CT-2004-511995, SYNSCAFF), Centre National de la Recherche Scientifique, Institut National de la Santé et de la Recherche Médicale, Agence Nationale de la Recherche, Région Languedoc Roussillon, and Canadian Institute of Health and Research. M.B. holds a Canada Research Chair in Signal Transduction and Molecular Pharmacology.

REFERENCES

1. Piehler, J. 2005. New methodologies for measuring protein interactions in vivo and in vitro. *Curr. Opin. Struct. Biol.* 15:4–14.
2. Giepmans, B. N., S. R. Adams, M. H. Ellisman, and R. Y. Tsien. 2006. The fluorescent toolbox for assessing protein location and function. *Science.* 312:217–224.
3. Eidne, K. A., K. M. Kroeger, and A. C. Hanyaloglu. 2002. Applications of novel resonance energy transfer techniques to study dynamic hormone receptor interactions in living cells. *Trends Endocrinol. Metab.* 13:415–421.
4. Hebert, T. E., C. Gales, and R. V. Rebois. 2006. Detecting and imaging protein-protein interactions during G protein-mediated signal transduction in vivo and in situ by using fluorescence-based techniques. *Cell Biochem. Biophys.* 45:85–109.
5. Lippincott-Schwartz, J., and G. H. Patterson. 2003. Development and use of fluorescent protein markers in living cells. *Science.* 300:87–91.
6. Tsien, R. Y., B. J. Bacskai, and S. R. Adams. 1993. FRET for studying intracellular signalling. *Trends Cell Biol.* 3:242–245.
7. Wu, P., and L. Brand. 1994. Resonance energy transfer: methods and applications. *Anal. Biochem.* 218:1–13.
8. Boute, N., R. Jockers, and T. Issad. 2002. The use of resonance energy transfer in high-throughput screening: BRET versus FRET. *Trends Pharmacol. Sci.* 23:351–354.
9. Ayoub, M. A., C. Couturier, E. Lucas-Meunier, S. Angers, P. Fossier, M. Bouvier, and R. Jockers. 2002. Monitoring of ligand-independent dimerization and ligand-induced conformational changes of melatonin receptors in living cells by bioluminescence resonance energy transfer. *J. Biol. Chem.* 277:21522–21528.
10. Erickson, M. G., B. A. Alseikhan, B. Z. Peterson, and D. T. Yue. 2001. Preassociation of calmodulin with voltage-gated Ca^{2+} channels revealed by FRET in single living cells. *Neuron.* 31:973–985.
11. Gordon, G. W., G. Berry, X. H. Liang, B. Levine, and B. Herman. 1998. Quantitative fluorescence resonance energy transfer measurements using fluorescence microscopy. *Biophys. J.* 74:2702–2713.
12. Wallrabe, H., and A. Periasamy. 2005. Imaging protein molecules using FRET and FLIM microscopy. *Curr. Opin. Biotechnol.* 16:19–27.
13. Nagoshi, E., C. Saini, C. Bauer, T. Laroche, F. Naef, and U. Schibler. 2004. Circadian gene expression in individual fibroblasts: cell-autonomous and self-sustained oscillators pass time to daughter cells. *Cell.* 119:693–705.
14. Hoshino, H., Y. Nakajima, and Y. Ohmiya. 2007. Luciferase-YFP fusion tag with enhanced emission for single-cell luminescence imaging. *Nat. Methods.* 4:637–639.
15. Loening, A. M., A. M. Wu, and S. S. Gambhir. 2007. Red-shifted *Renilla reniformis* luciferase variants for imaging in living subjects. *Nat. Methods.* 4:641–643.
16. Xu, X., M. Soutto, Q. Xie, S. Servick, C. Subramanian, A. G. von Arnim, and C. H. Johnson. 2007. Imaging protein interactions with bioluminescence resonance energy transfer (BRET) in plant and mammalian cells and tissues. *Proc. Natl. Acad. Sci. USA.* 104:10264–10269.
17. De, A., A. M. Loening, and S. S. Gambhir. 2007. An improved bioluminescence resonance energy transfer strategy for imaging intracellular events in single cells and living subjects. *Cancer Res.* 67:7175–7183.
18. Hamdan, F. F., M. Audet, P. Garneau, J. Pelletier, and M. Bouvier. 2005. High-throughput screening of G protein-coupled receptor antagonists using a bioluminescence resonance energy transfer 1-based β-arrestin2 recruitment assay. *J. Biomol. Screen.* 10:463–475.
19. Kalderon, D., B. L. Roberts, W. D. Richardson, and A. E. Smith. 1984. A short amino acid sequence able to specify nuclear location. *Cell.* 39: 499–509.
20. Perroy, J., S. Pontier, P. G. Charest, M. Aubry, and M. Bouvier. 2004. Real-time monitoring of ubiquitination in living cells by BRET. *Nat. Methods.* 1:203–208.
21. Perroy, J., L. Adam, R. Qanbar, S. Chenier, and M. Bouvier. 2003. Phosphorylation-independent desensitization of GABA(B) receptor by GRK4. *EMBO J.* 22:3816–3824.
22. Pfleger, K. D., and K. A. Eidne. 2006. Illuminating insights into protein-protein interactions using bioluminescence resonance energy transfer (BRET). *Nat. Methods.* 3:165–174.
23. Mercier, J. F., A. Salahpour, S. Angers, A. Breit, and M. Bouvier. 2002. Quantitative assessment of β 1- and β 2-adrenergic receptor homo- and heterodimerization by bioluminescence resonance energy transfer. *J. Biol. Chem.* 277:44925–44931.
24. Oakley, R. H., S. A. Laporte, J. A. Holt, L. S. Barak, and M. G. Caron. 1999. Association of β-arrestin with G protein-coupled receptors during clathrin-mediated endocytosis dictates the profile of receptor resensitization. *J. Biol. Chem.* 274:32248–32257.
25. Laporte, S. A., R. H. Oakley, J. A. Holt, L. S. Barak, and M. G. Caron. 2000. The interaction of β-arrestin with the AP-2 adaptor is required for the clustering of β 2-adrenergic receptor into clathrin-coated pits. *J. Biol. Chem.* 275:23120–23126.
26. Vrecl, M., R. Jorgensen, A. Pogacnik, and A. Heding. 2004. Development of a BRET2 screening assay using β-arrestin 2 mutants. *J. Biomol. Screen.* 9:322–333.
27. Charest, P. G., and M. Bouvier. 2003. Palmitoylation of the V2 vasopressin receptor carboxyl tail enhances β-arrestin recruitment leading to efficient receptor endocytosis and ERK1/2 activation. *J. Biol. Chem.* 278:41541–41551.